Hindawi
Wireless Communications and Mobile Computing
Volume 2022, Article ID 6144741, 10 pages
https://doi.org/10.1155/2022/6144741

Research Article

Energy-Efficient Resource Allocation for Backscatter-Assisted Wireless Powered Communication Networks in Twin Workshop

Yujian Li and Xinxing Zhang

Department of Mechanical and Electrical Engineering, Quzhou College of Technology, China

Correspondence should be addressed to Xinxing Zhang; redrobot@zjut.edu.cn

Received 1 March 2022; Revised 14 April 2022; Accepted 22 April 2022; Published 19 May 2022

Academic Editor: Yinghui Ye

The problem of energy shortage in sensor nodes caused by frequent data interactions is one of the major constraints on the development of twin workshops. A backscatter-assisted wireless powered communication network (BAWPCN) has been deemed a potential solution for addressing the problem of energy shortage in twin workshops. How to effectively ensure the link energy efficiency (EE) while satisfying the quality of servers for each user has been of high interest, while it has not been well studied in previous works. Inspired by this, in this paper, we propose a resource allocation scheme based on the max–min criterion, considering the user quality of service and energy-causality constraints. The optimization problem is formulated as a mixed-integer nonconvex fractional planning problem which is aimed at maximizing the minimum EE of each link. The generalized fractional theory is used to transform the nonconvex fractional planning problem into an equivalent mixed-integer nonconvex subtraction optimization problem, and then, the mixed-integer nonconvex subtractive optimization problem is transformed into an equivalent nonconvex optimization problem by introducing relaxation variables to eliminate the integer programming problem arising from the maximum-minimum function. Based on this, the block coordinate descent method is used to decompose the transformation problem into two convex subproblems, and an iterative algorithm is proposed to solve the transformation problem. Simulation results verify the fast convergence of the proposed iterative algorithm and show that the proposed resource allocation method can effectively guarantee the fairness of the energy efficiency of the system in twin workshops.

1. Introduction

Industry 4.0 refers to using the Cyberphysical System (CPS) to digitize and intellectualize the supply, manufacturing, and sales information in production and finally achieves fast, effective, and personalized product supply. The core of Industry 4.0 is the interconnection and intelligent operation of the physical and information worlds of manufacturing. The combination of intelligent automation (e.g., robotics) and a new generation of information technology (e.g., Internet of Things and artificial intelligence) produces the digital twin workshop, which is one of the current trends in manufacturing in the context of Industry 4.0 [1]. Digital twin (DT) is driven by the multidimensional virtual model and fused data and realizes monitoring, simulation, prediction, optimization, and other actual functional services and application requirements through virtual and real closed-loop interaction [2], as shown in Figure 1. Digital twin workshops (DTW), as an important enabling way to realize digital transformation, promote intelligent upgrading, and accelerate Industry 4.0, have moved from theoretical research to the practical application stage, among which the development of Internet of Things technology is the key driving force.

With the development of Internet of Things (IoT) technology and its wide application in the manufacturing industry, it greatly enhances the real-time data acquisition ability and the transmission ability of production factors in twin workshops. The realization of ubiquitous IoT requires the deployment of numerous low-power sensors, but the frequent data interaction

will greatly consume sensor energy [4]. One way to solve the problem is replacing the battery, but the deployment of sensors in an industrial production environment cannot meet the demand to frequently replace the battery. At the same time, as the power consumption and volume of wireless sensor nodes become smaller and smaller, the advantages of small and flexible wireless sensor nodes will be limited if they only rely on their own power supply. Therefore, the energy shortage of sensor nodes caused by frequent data interaction is one of the important factors restricting the development of twin workshops. In recent years, thanks to the progress of science and technology, scholars have proposed wireless power communication network (WPCN) and backscatter communication technologies to solve the energy limitation problem of sensor nodes. The WPCN deploys dedicated energy stations to provide the energy resource to the sensor nodes through the wireless energy transfer (WET) technology, and the nodes leverage the harvested energy to transmit information. Therefore, the core of WPCN design lies in the joint allocation of energy and time resource. The authors in [5] proposed the harvest-then-transmit (HTT) protocol by incorporating WET into wireless communication networks, which is the main basis for the operation of current WPCNs. In [6], the half-duplex mode is extended to the full-duplex mode, and the base station contains two antennas so that it can simultaneously transmit energy signals and receive transmission data. However, the transmitter performs active transmission (AT) by the HTT protocol, which leads to high power consumptions. Thus, the transmitter has to allocate a long period to harvest sufficient energy but leaves a short period to transmit information. Backscatter communication (BackCom) technology adopts a relatively simple modulation method to load its information to external RF signals for transmission. Thus, BackCom avoids power-consuming components, providing a transmission strategy with low power consumption and low transmission rate for IoT scenarios [7]. The long period for HTT to harvest energy is available for BackCom to increase the throughput. Thus, BackCom can be combined with HTT to achieve different tradeoffs between energy harvesting (EH) and data transmission.

The authors of [8] take the wireless digital TV signal as an example to show that the sensor can maintain communication by using the existing wireless signal without batteries. In [9, 10], the authors combined BackCom with WPCN and proposed a backscatter-assisted wireless powered communication network (BAWPCN). For the BAWPCNs, the authors of [11] considered a network combining multimode backscatter communication and HTT and proposed a time slot resource allocation scheme to maximize subuser link capacity. In [12], the authors studied the optimal time allocation of energy harvesting, backscatter, and wireless transmission to maximize the throughput. The authors of [13] proposed a resource allocation scheme to maximize the throughput by jointly optimizing the transmission time, reflection coefficient, and transmit power in the full-duplex BackCom. The authors of [14] considered the scenario of nonorthogonal multiple access and maximized the throughput by jointly optimizing the backscatter time and reflection coefficient, subject to the constraints of energy collection threshold and signal-to-noise ratio. Energy efficiency (EE) is also one of the important indicators of wireless communication networks; the authors in [15] studied the resource allocation method to maximize the user EE in the BAWPCNs. Then, users' EE was also studied in an unmanned aerial vehicle-based WPCN with backscatter communications [16]. Based on the analysis of existing literature, it can be seen that there are many researches on BAWPCNs from the evaluation of network outage capacity or spectral efficiency, while there are few researches from the perspective of energy efficiency. Meanwhile, the following three problems still exist in the research process: (1) there are only single nodes in BackCom; (2) only the time dimension is considered in the design of resource allocation, while the power resource allocation is ignored; and (3) the energy harvesting model adopts the linear mode. However, in the case of a multiuser network in the twin workshop, the communication network composed of multiple nodes should be considered. A large number of nonlinear components such as photoelectric sensors and Hall sensors are used in twin workshops, and the actual energy harvesting circuit presents nonlinear characteristics. At the same time, power resources also affect the level of energy efficiency. Inspired by the above three problems, aiming at the energy shortage caused by frequent data exchange of each sensor node in the twin workshop, this paper introduces a BAWPCN to study the time-power two-dimension resource allocation method for multiple users and optimize the energy efficiency of the communication link. Our main contributions are summarized as follows.

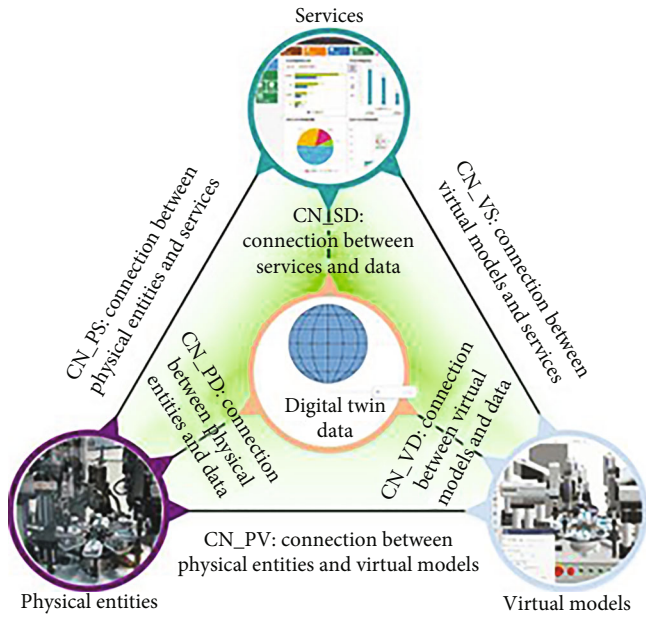

Figure 1: Digital twin model [3].

(i) A joint energy efficiency/fairness time-power two-dimensional resource optimization model for the system based on the max–min criterion is proposed. The proposed optimization model not only ensures fair access to communication resources for users but also considers the optimization of the time slot, transmit power of the power beacon, and nodes simultaneously

(ii) The joint optimization of time slot and power leads to coupling of multiple variables and a fractional form of the objective function. In addition, there is a max–min function of the objective function. The proposed optimization model is therefore a mixed-integer nonconvex fractional programming problem and cannot be solved directly using the existing tools such as CVX

(iii) The proposed iterative algorithm is verified to converge quickly through simulation and is shown to achieve better fairness of the link EE when compared with similar algorithms

The rest of this paper is organized as follows. In Section 2, the system model for BAWPCN is introduced. In Section 3, we formulate the problem to maximize the minimum links' EE and solve it for the EE fairness resource allocation scheme. In Section 4, the simulations are conducted to evaluate the performance of the proposed scheme. Section 5 concludes this paper.

2. System Model

Consider a BAWPCN as shown in Figure 2, the network consists of a gateway (GW) to receive information, a dedicated power beacon (PB) to provide energy, and M power-limited users (EUs).

The EUs need to upload their data to the gateway within time slot T. The PB was deployed to provide radio frequency (RF) signals to EUs who can use the received RF signals for backscatter communication and energy harvesting.

In order to avoid interference between EUs, time division multiple access is adopted to decompose the whole time slot T into multiple small time slots, as shown in Figure 2. In αT, PB broadcasts the unmodulated RF signals, and all EUs can use the received RF signals for energy harvesting or backscatter information. Specifically, in τ_0, all EUs work in the energy harvesting mode. At the time slot τ_m $(m = 1, 2, \cdots, M)$, EU m transmits data to the GW through backscatter technology while the other EUs continue to harvest energy. In $(1-\alpha)T$, the PB remains silent and EU m transmits its data to the GW in slot τ_m by active communication. The signal received by the mth EU in αT can be expressed as

$$y_m^{\tau_0} = w_m + \sqrt{P_0} g_m x, \tag{1}$$

where P_0 represents the transmitted power of the PB, x denotes RF signals transmitted by PB and $E[|x|^2] = 1$, w_m represents the receiving noise of mth EU and follows a Gaussian distribution with the mean of 0 and variance of σ^2, and g_m represents the channel coefficient from PB to mth EU. Using the nonlinear energy harvesting model proposed in [17], the energy harvested by EU m within time slot αT can be expressed as follows:

$$\Phi_m^{\text{total}}(P_0, \alpha, \tau_m) = (\alpha T - \tau_m) E_{\max} \frac{1 - \exp\left(-cP_0|g_m|^2\right)}{1 + \exp\left(-cP_0|g_m|^2 + cd\right)}, \tag{2}$$

where $E_{\max}$ is the maximum harvested power of the energy collector, c and d are parameters of the nonlinear energy model, and their values can be obtained by fitting the actual measured data. Since the value of harvested energy is positive, the value of c must meet the requirement $1 - \exp\left(-cP_0|g_m|^2\right) > 0$. It should be noted that the time for EU m to harvest energy is $(\alpha T - \tau_m)$, not αT, because EU m operates in the backscattering communication mode within the τ_m time slot. It should be pointed out that the energy collected in formula (2) will be used for mth EU's backscatter communication and HTT energy dissipation in τ_m and t_m time slots. In τ_m, EU m backscatters information to the gateway via the backscattering communication technique, where the instantaneous power of the reflected signal received by the gateway from mth EU can be expressed as

$$P_{\tau_m}(P_0) = \frac{4P_0|g_m|^2|h_m|^2\varepsilon^2(\Gamma_0 - \Gamma_1)^2}{\pi^2}, \tag{3}$$

where ε is the scattering efficiency of the backscattering communication module, h_m denotes the channel coefficient from mth EU to the gateway, and Γ_0 and Γ_1 denote the reflection coefficient. The Fries transfer formula is used to model the channel gain, $|g_m|^2 = G_p G_h \lambda^2/(4\pi d_{0m})^2$, $|h_m|^2 = G_h G_r \lambda^2/(4\pi d_{1m})^2$, where λ denotes the wavelength; G_p, G_h, G_r denote the antenna gain of the PB, the EUs, and the gateway, respectively; and d_{0m} and d_{1m} denote the distance from the PB to m th EU and mth EU to the gateway, respectively. According to Equation (3) and Shannon's capacity theorem, the achievable throughput of mth EU at τ_m can be calculated as follows:

$$C_{\tau_m}^{\text{Back}}(\tau_m, P_0) = B_0 \tau_m \log_2\left(1 + \frac{\xi P_{\tau_m}(P_0)}{\sigma^2}\right), \tag{4}$$

where B_0 denotes bandwidth. Since backscatter communication uses simple modulation, its channel capacity is smaller than that of conventional communication modes. In this paper, we use the same approach as in [18] to characterize this difference in channel capacity, i.e., multiplying the signal reception signal-to-noise ratio by a nonnegative real number ζ with a factor less than 1 $(0 < \zeta < 1)$. In $(1-\alpha)T$, mth EU transmits data to the gateway in time slot t_m in the traditional communication mode, so the throughput that mth EU can accomplish is expressed as

$$C_{t_m}^{\text{HTT}}(t_m, P_{t_m}) = B_0 t_m \log_2\left(1 + \frac{P_{t_m}|h_m|^2}{\sigma^2}\right), \tag{5}$$

where P_{t_m} denotes the transmit power of mth EU during time slot t_m. Thus, the total throughput by mth EU during the entire time slot T can be expressed as

$$C_m^{\text{total}}(\tau_m, t_m, P_{t_m}, P_0) = B_0\left(\tau_m \log_2\left(\left(1 + \frac{\xi P_{\tau_m}(P_0)}{\sigma^2}\right) + t_m \log_2\left(1 + \frac{P_{t_m}|h_m|^2}{\sigma^2}\right)\right)\right). \tag{6}$$

According to Equation (18) in [19], the EU EE is the ratio of

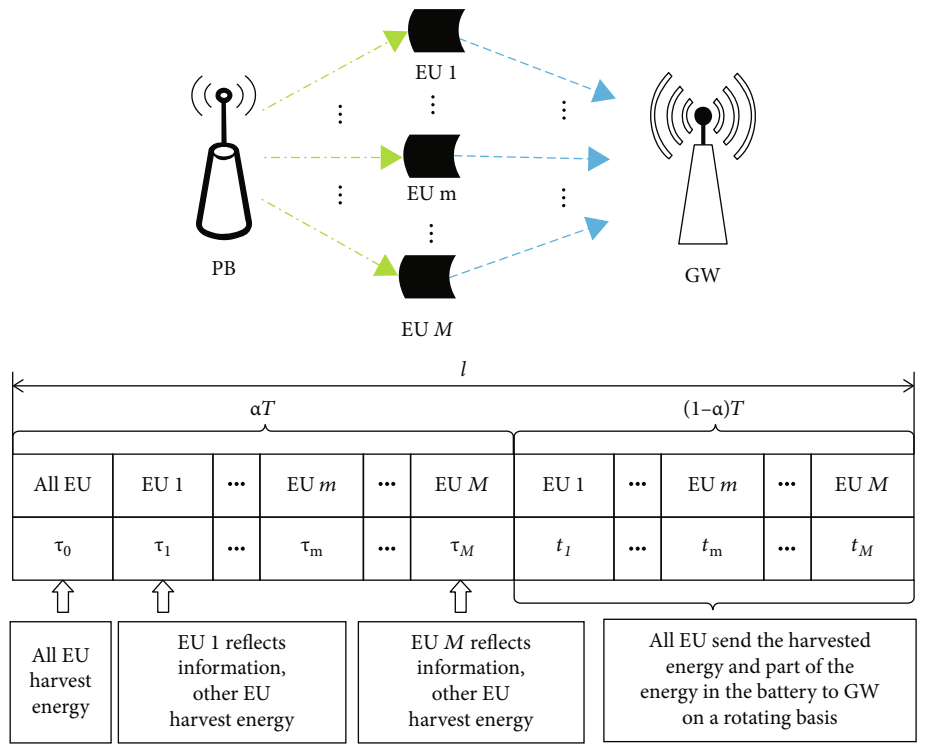

Figure 2: System model.

the total throughput achieved by the user to the consumed energy. Equation (6) already gives the total throughput that can be completed by user m throughout the time slot. Next, this section analyses the energy consumed by mth EU throughout the time slot and the expression of EE.

During time slots τ_0 and τ_m, mth EU collects energy from a dedicated energy station. During time slots τ_m and t_m, the mth EU needs to consume energy. During time slot τ_m, there is only circuit loss as the mth EU modulates its own information to the received RF signal (i.e., the RF signal emitted by the energy source) and does not need to generate its own carrier. During time slot t_m, the mth EU uses a conventional communication mode to transmit data, so its energy consumption consists of two components: the energy consumed by the transmit power and the circuit losses. In summary, the total system energy consumed by mth EU is

$$E_m^{\text{total}}\left(\tau_m, t_m, P_{t_m}, P_0\right) = P_0(\tau_0 + \tau_m) + \left(p_{m,c}^{\text{HTT}} + P_{t_m}\right)t_m + p_{m,c}^{\text{Back}}\tau_m, \tag{7}$$

where $p_{m,c}^{\text{Back}}$ denotes the circuit loss when mth EU operates in the backscatter communication mode, $p_{m,c}^{\text{HTT}}$ denotes the circuit loss when mth EU is operating in the conventional communication mode, and P_{t_m} denotes the transmit power of m th EU in time slot t_m.

Combining Equations (6) and (7), the link EE of mth EU can be expressed as

$$\eta_m\left(\tau_m, t_m, P_{t_m}, P_0\right) = \frac{C_m^{\text{total}}\left(\tau_m, t_m, P_{t_m}, P_0\right)}{E_m^{\text{total}}\left(\tau_m, t_m, P_{t_m}\right)}. \tag{8}$$

3. Resource Allocation Method for Energy Efficiency Fairness of the System

3.1. Problem Formulation. In this subsection, we propose a resource allocation scheme that can effectively guarantee the EE fairness of communication links. The max–min criterion is an effective way to guarantee user fairness [20], so that the resource allocation method for guaranteeing energy-efficient fairness of links among EUs can be achieved by solving the following optimization problem, namely,

$$\begin{aligned}
&\max_{\{\tau_m\},\{t_m\},\left\{P_{t_m}\right\},P_0,\beta,\tau_0} \min_m \eta_m\left(\tau_m, t_m, P_{t_m}, P_0\right),\\
&\text{C1}: \tau_0 + \sum_{m=1}^{M}\tau_m \le \alpha T,\\
&\text{C2}: \sum_{m=1}^{M} t_m \le (1-\alpha)T,\\
&\text{C3}: p_{m,c}^{\text{Back}}\tau_m + \left(p_{m,c}^{\text{HTT}} + P_{t_m}\right)t_m \le \Phi_m^{\text{total}}(P_0, \alpha, \tau_m), \forall m,\\
&\text{C4}: 0 \le P_{t_m} \le P_m^{\max}, \forall m,\\
&\text{C5}: C_m^{\text{total}}\left(\tau_m, t_m, P_{t_m}, P_0\right) \ge C_m^{\min}, \forall m,\\
&\text{C6}: 0 \le P_0 \le P_0^{\max},\\
&\text{C7}: \tau_0 > 0, \tau_m \ge 0, t_m \ge 0, \forall m.
\end{aligned} \tag{9}$$

C3 ensures that the harvested energy is greater than the energy consumed by user m. C4 constrains the maximum

transmit power of the mth EU when working in the traditional information transmission mode. C5 indicates that the throughput achieved by mth EU in the whole time slot T cannot be less than the given minimum value, i.e., the communication service quality of user m is guaranteed. C6 constrains the maximum transmit power of the PB.

As can be seen from the objective function, the EE of m th link η_m is a fraction function, which contains multiple coupled variables, such as the variables P_{tm} and t_m, P_0, τ_0, and τ_m. Secondly, since the max–min criterion is adopted, the integer variable M needs to be optimized. Therefore, the optimization problem (9) is a mixed-integer nonconvex fractional programming optimization problem. Therefore, the existing optimization tools such as CVX cannot be directly used to solve the original problem.

3.2. Problem Transformation. For the mixed-integer nonconvex fractional programming problem in Equation (9), we divide three steps to obtain its optimal solution. Firstly, the nonconvex fractional programming problem is transformed into an equivalent mixed-integer nonconvex subtractive optimization problem by using the generalized fractional programming theory. Secondly, the integer programming problem caused by the max–min function is eliminated by introducing relaxation variables; that is, the mixed-integer nonconvex subtraction optimization problem is transformed into an equivalent nonconvex optimization problem. Finally, the block coordinate descent (BCD) technology was used to decompose the transformation problem into two convex subproblems [21], and then, an iterative algorithm was designed to solve the transformation problem.

The BCD algorithm encompasses a wider range of traditional alternating optimization algorithms as well as coordinate descent algorithms. The BCD algorithm is usually applied to optimization problems with nonconvex objective functions or feasible domains, but when the optimization variables are blocked, the objective functions and feasible domains of such optimization problems are convex with respect to the blocks of variables. In addition, the scope of the BCD algorithm can be extended, for example, by using approximate optimization for nonconvex objective functions and feasible domains after blocking the variables, where the BCD algorithm is also feasible [22].

The specific processing steps are described below.

(1) Let the variable Q denote the value of the objective function of problem (9), i.e., the max–min EE. According to the generalized fractional programming theory, the sufficient condition for obtaining the optimal solution to the optimization problem (9) is that Equation (10) holds when the C1-C7 constraints are satisfied:

$$\max_{\{\tau_m\},\{t_m\},\{P_{t_m}\},P_0,\beta,\tau_0} \min_m C_m^{\text{total}}\left(\tau_m, t_m, P_{t_m}, P_0\right) - Q * E_m^{\text{total}}\left(\tau_m, t_m, P_{t_m}\right) = \min_m \left[C_m^{\text{total}}\left(\tau_m^*, t_m^*, P_{t_m}^*, P_0^*\right) - Q * E_m^{\text{total}}\left(\tau_m^*, t_m^*, P_{t_m}^*\right)\right] = 0. \tag{10}$$

We can obtain the optimal solution to the original problem by solving the optimization problem (10). However, in practice, Q^* is often unknown, but we can obtain Q by continuously updating the value of Q^*, which is shown in Algorithm 1.

According to Algorithm 1, the core of solving the original problem (9) is to solve the optimization problem. Compared to the original problem (9), the objective function of optimization problem does not have a fractional form, but it is still a mixed-integer nonconvex optimization problem.

(2) A relaxation variable is introduced to transform the mixed-integer nonconvex optimization problem into the following optimization problem, namely,

$$\begin{aligned} &\max_{\{\tau_m\},\{t_m\},\{P_{t_m}\},P_0,\alpha,\tau_0} \theta \\ &\text{s.t.C1} - \text{C7}, \\ &\text{C8}: C_m^{\text{total}}\left(\tau_m, t_m, P_{t_m}, P_0\right) - QE_m^{\text{total}}\left(\tau_m, t_m, P_{t_m}\right) \geq \theta, \forall m. \end{aligned} \tag{11}$$

In the optimization problem (11), the optimization objective is a linear function and the constraints C1, C2, C4, C6, and C7 are linear constraints, but the remaining constraints C3, C5, and C8 are nonconvex, so the optimization problem (11) is a nonconvex problem.

(3) The optimization problem (11) is transformed into two subproblems using the BCD technique as follows:

(1) Given $P_0^{(l)}$, solve for $\tau_m^{(l)}$, $t_m^{(l)}$, $P_{t_m}^{(l)}$, $\tau_0^{(l)}$, $\alpha^{(l)}$ by the following problem:

$$\begin{aligned} &\max_{\{\tau_m\},\{t_m\},\{P_{t_m}\},\alpha,\tau_0} \theta \\ &\text{s.t.C1, C2, C4, C7}, \\ &\text{C3}: p_{m,c}^{\text{Back}}\tau_m + \left(p_{m,c}^{\text{HTT}} + P_{t_m}\right)t_m \leq \Phi_m^{\text{total}}\left(P_0^{(l)}, \alpha, \tau_m\right), \forall m, \\ &\text{C5}: C_m^{\text{total}}\left(\tau_m, t_m, P_{t_m}, P_0^{(l)}\right) \geq C_m^{\min}, \forall m, \\ &\text{C6}: 0 \leq P_0^{(l)} \leq P_0^{\max}, \\ &\text{C8}: C_m^{\text{total}}\left(\tau_m, t_m, P_{t_m}, P_0^{(l)}\right) - QE_m^{\text{total}}\left(\tau_m, t_m, P_{t_m}, P_0^{(l)}\right) \geq \theta, \forall m. \end{aligned} \tag{12}$$

In the optimization problem (12), constraints C3, C5, and C8 still exist in the coupled variable and are jointly nonconvex. Specifically, in C3 and C8, the variable P_{t_m} and t_m are coupled; in C5 and C8, the joint nonconvexity is present in $t_m \log_2(1 + P_{t_m}|h_m|^2/\sigma^2)$. To solve the above problem, we introduce auxiliary variable $x_m = P_{t_m} t_m$ and bring them into

$$\begin{aligned}
&\max_{\{\tau_m\},\{t_m\},\{x_m\},\alpha,\tau_0} \theta \\
&\text{s.t.C1, C2, C7,} \\
&\text{C3}: p_{m,c}^{\text{Back}}\tau_m + p_{m,c}^{\text{HTT}}t_m + x_m \le \Phi_m^{\text{total}}\left(P_0^{(l)}, \alpha, \tau_m\right), \forall m, \\
&\text{C4}: 0 \le x_m \le P_m^{\max}t_m, \\
&\text{C5}: B_0\tau_m \log_2\left(\left(1 + \frac{\xi P_{\tau_m}\left(P_0^{(l)}\right)}{\sigma^2}\right)\left(1 + \frac{x_m|h_m|^2}{t_m\sigma^2}\right)\right) \ge C_m^{\min}, \forall m, \\
&\text{C6}: 0 \le P_0^{(l)} \le P_0^{\max}, \\
&\text{C8}: B_0\tau_m \log_2\left(\left(1 + \frac{\xi P_{\tau_m}\left(P_0^{(l)}\right)}{\sigma^2}\right)\left(1 + \frac{x_m|h_m|^2}{t_m\sigma^2}\right)\right) - Q\left(P_0^{(l)}(\tau_0 + \tau_m) + p_{m,c}^{\text{Back}}\tau_m + p_{m,c}^{\text{HTT}}t_m + x_m\right) \ge \theta, \forall m.
\end{aligned} \tag{13}$$

the optimization problem (13) to obtain the equivalent optimization problem as follows, i.e.,

(2) Given $\tau_m^{(l)}$, $t_{m^{(l)}}$, $P_{t_m}^{(l)}$, $\tau_0^{(l)}$, $\alpha^{(l)}$, we can obtain $P_0^{(l)}$ by solving the following optimization problem:

$$\begin{aligned}
&\max_{P_0} \theta \\
&\text{s.t.C1}: \tau_0^{(l)} + \sum_{m=1}^{M} \boxtimes\tau_m^{(l)} \le \alpha^{(l)}T, \\
&\text{C2}: \sum_{m=1}^{M} \boxtimes t_m^{(l)} \le \left(1 - \alpha^{(l)}\right)T, \\
&\text{C3}: p_{m,c}^{\text{Back}}\tau_m^{(l)} + p_{m,c}^{\text{HTT}}t_m^{(l)} + x_m^{(l)} \le \Phi_m^{\text{total}}\left(P_0, \alpha^{(l)}, \tau_m^{(l)}\right), \forall m, \\
&\text{C4}: 0 \le x_m^{(l)} \le P_m^{\max}t_m^{(l)}, \\
&\text{C5}: B_0\tau_m^{(l)} \log_2\left(\left(1 + \frac{\xi P_{\tau_m}(P_0)}{\sigma^2}\right)\left(1 + \frac{x_m^{(l)}|h_m|^2}{t_m^{(l)}\sigma^2}\right)\right) \ge C_m^{\min}, \forall m, \\
&\text{C6}: 0 \le P_0 \le P_0^{\max}, \\
&\text{C7}: \tau_0^{(l)} > 0, \tau_m^{(l)} \ge 0, t_m^{(l)} \ge 0, \forall m, \\
&\text{C8}: B_0\tau_m^{(l)} \log_2\left(\left(1 + \frac{\xi P_{\tau_m}(P_0)}{\sigma^2}\right)\left(1 + \frac{x_m^{(l)}|h_m|^2}{t_m^{(l)}\sigma^2}\right)\right) - Q\left(P_0\left(\tau_0^{(l)} + \tau_m^{(l)}\right) + p_{m,c}^{\text{Back}}\tau_m^{(l)} + p_{m,c}^{\text{HTT}}t_m^{(l)} + x_m^{(l)}\right) \ge \theta, \forall m.
\end{aligned} \tag{14}$$

Lemma 1. *The optimization problem (13) is a convex problem.*

Proof. Please see the appendix.

According to Lemma 1, we can use the CVX tool to obtain the optimal solution to solve the optimization problem (13). □

In the optimization problem (14), the objective function is linear and C1, C2, C4, and C7 are independent of the optimization variables. C6 is a linear constraint. Meanwhile, C3 and C5 are convex constraints. The left-hand side of C8 is shaped as $f(x) = C\log_2(1 + Dx) - ax + b$, where a, b, C, and D are all constants and greater than zero. The second-

1: Solve the optimal solution of the optimization problem given any Q greater than zero
2: Substitute the optimal solution obtained in the first step into the objective function of the optimization problem (9) to update $Q(0)$
3: If Q does not converge, let $Q = Q(0)$ and repeat the first step; if not, let $Q^* = Q$, and the optimal solution in the first step is the optimal solution of the original problem (9):

$$\max_{\{\tau_m\},\{t_m\},\{P_{t_m}^{(2)}\},P_0,\alpha,\tau_0} \min_m C_m^{\text{total}}(\tau_m, t_m, P_{t_m}, P_0) - QE_m^{\text{total}}(\tau_m, t_m, P_{t_m})$$

s.t.C1 − C7

Algorithm 1: The link EE fairness resource allocation algorithm.

1: Initialize the system parameters, given $P_0^{(l)}$, the convergence accuracy δ, and the maximum iteration number L
2: Repeat
3: For given $P_0^{(l)}$, solve the problem (13) by using CVX to obtain $\tau_m^{(l+1)}$, $t_m^{(l+1)}$, $x_m^{(l+1)}$, $\tau_0^{(l+1)}$, α^{l+1}
4: For given $\tau_m^{(l+1)}$, $t_m^{(l+1)}$, $x_m^{(l+1)}$, $\tau_0^{(l+1)}$, α^{l+1}, solve the problem (14) by using CVX to obtain $P_0^{(l+1)}$
5: Until $\theta^{(l+1)} - \theta^{(l)} \le \delta$ or $l = L$
6: Return the optimal solutions: $\tau_m^* = \tau_m^{(l+1)}$, $t_m^* = t_m^{(l+1)}$, $\tau_0^* = \tau_0^{(l+1)}$, $\alpha^* = \alpha^{(l+1)}$, $P_{t_m}^* = P_{t_m}^{(l+1)}$, $P_0^* = P_0^{(l+1)}$

Algorithm 2: Iterative algorithm for solving optimization problem.

1: Given any $Q^{(0)}$ greater than zero, use Algorithm 2 to obtain an optimal solution to the optimization problem (14)
2: Update Q by bringing the optimal solution obtained in the first step into the objective function of the optimization problem (9)
3: If Q does not converge, let $Q^{(0)} = Q$ and repeat the first step; if not, let $Q^* = Q$, and the solution obtained in the first step is the solution to the original problem (9)

Algorithm 3: The overall algorithm of link EE fairness resource allocation scheme.

order derivative of $f(x)$ can be calculated as $f''(x) = -CD^2/(1+Dx)^2 \ln 2$. $f''(x) < 0$, so C8 is a convex constraint. Therefore, the optimization problem (14) is convex, and we can use the CVX tool to obtain the optimal solution to the optimization problem (14).

Based on the above analysis, the optimization problem can be solved by an iterative BCD-based algorithm, as described in Algorithm 2.

As the optimization problems (13) and (14) are convex, the convergence of Algorithm 2 is guaranteed [23]. The overall algorithm of the link energy efficiency fairness resource allocation scheme can be described as Algorithm 3.

4. Simulation Results and Analysis

In this section, we provide simulation results to evaluate the performance of the proposed iterative algorithm. In addition, we illustrate the advantages of the proposed resource allocation scheme based on the max–min criterion to guarantee energy efficiency fairness by comparing with the total energy efficiency maximization scheme. Unless otherwise stated, the parameters listed in Table 1 are used in this section. In addition, the distance between the gateway and the PB is assumed to be 52 m; the distance between the three EUs and the PB is 1.8 m, 1.6 m, and 1.4 m, respectively. Based on the simulated channel gains $|g_m|^2$ and $|h_m|^2$ and the energy harvesting circuits, dedicated power stations produced by the powercast company, the antenna gains of the PB and gateways assume as 5 dBi, and the antenna gain of each EU is 2 dBi in this paper. Assume a carrier frequency of 915 MHz.

The convergence performance of the proposed resource allocation algorithm is shown in Figure 3. It can be seen that the proposed iterative algorithm converges to a certain constant after roughly three to four iterations, which validates the fast convergence of Algorithm 1. Secondly, we can see that ζ has an important influence on the energy efficiency of the system link. As in Equation (4), the max–min EE should increase with the ζ. And we can see that the larger the ζ, the greater the max–min EE from the figure.

Figure 4 shows the achieved EE versus the performance gap ζ. We compare the max–min link EE achieved by the proposed transmission strategy and the transmission strategies of the HTT mode and backscatter communication mode. As can be seen in Figure 4, the proposed transmission strategy achieves the max–min link EE no worse than these

Table 1: Simulation parameter settings.

Parameters	Symbols	Value
The number of EUs	M	3
The maximum transmit power of PB	P_0	3 W
The entire transmission time slot	T	1 s
Bandwidth	B_0	10 MHz
Circuit loss in backscatter communication mode	$p_{m,c}^{\text{Back}}$	400 μW
The maximum transmit power of mth EU	P_{t_m}	10 mW
Circuit loss of transmitting information in HTT mode	$p_{m,c}^{\text{HTT}}$	1 mW
Reflection coefficient	Γ_0	1
Reflection coefficient	Γ_1	-1
Scattering efficiency of the backscatter communication module	ε	-1.1 dB

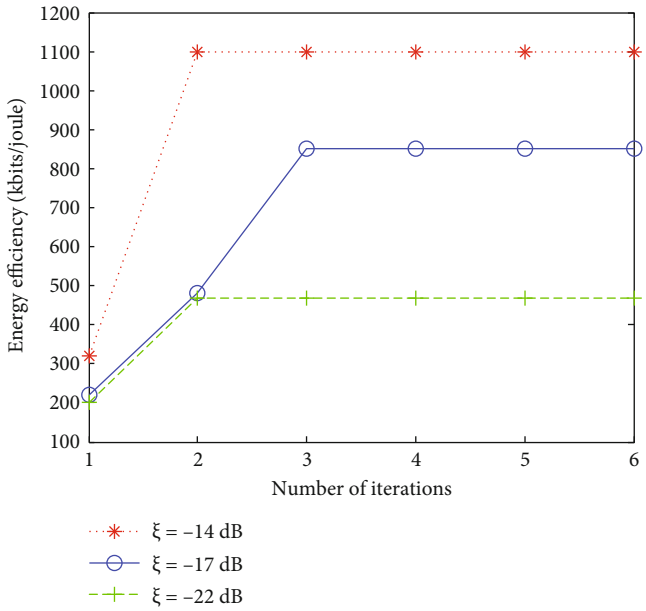

Figure 3: Convergence diagram for Algorithm 1.

transmission strategies regardless of the value of ζ. It is noted that the proposed hybrid transmission strategy can be degraded to these two transmission modes by adjusting parameters. It is consistent that the two transmission modes are special cases of the transmission strategy, and there is a tradeoff between the BackCom and HTT mode in the proposed resource allocation scheme as in theoretical analysis. Specifically, when ζ is less than or equal to -18 dB, the max–min link EE achieved by the proposed transmission strategy is the same as the max–min link EE in the HTT mode. When ζ is greater than -18 dB and less than -14 dB, the proposed transmission strategy makes EUs work in both backscatter and HTT modes in a full transmission time slot; when ζ is greater than -14 dB, it can be seen that the max–min EE accomplished by the proposed transmission strategy is the same as the max–min link EE in the backscatter communication mode, which means that when ζ is larger, the proposed transmission strategy degrades to the backscattered communication mode. In addition, compared to the throughput maximization resource allocation scheme, the EE by the proposed max–min fairness scheme presents better performance. The reason is that the throughput maximization scheme maximizing UE throughput in a BAWPCN does not take into account the factor of EE; the achieved EE is lower than that of the proposed max–min EE fairness scheme. The above analysis shows that the BAWPCNs can indeed combine the advantages of both backscatter and WPCNs, allowing them to adaptively adjust their parameters to meet the different communication goals in complex communication demands.

In Figure 5, we compare the total EE maximization resource allocation scheme with the proposed max–min link EE resource allocation scheme, under the case of large and small interuser channel differences. The major difference between the two resource allocation schemes is the objective function. According to Equation (9), the objective function is the minimum EE for the proposed max–min resource allocation scheme. For the total EE maximization resource allocation scheme, the objective function is the sum rates divided by the sum energy consumptions of M EUs calculated as $\sum_{m=1}^{M}$throughput of the mth SN/$\sum_{m=1}^{M}$energy of the mth SN. It can be seen that the difference in EE between the best and worst EUs under the total EE maximization resource allocation scheme is significantly greater than that of the proposed max–min resource allocation scheme. When the channel difference between users is small, the average EE of users under the total EE maximization resource allocation scheme is slightly higher than that under the proposed max–min resource allocation scheme, but the difference between the EE of the best and worst users is significantly higher than the proposed resource allocation scheme. When the channel difference between users is large, it can be seen that the EE by the total EE maximization scheme results in the energy efficiency of the best user being 2.2 times that of the worst link, but the EE of the best link is about 1.4 times that of the worst link by the proposed resource allocation scheme, which effectively ensures fair access to resources between EUs. This is because the total EE maximization resource allocation scheme inclines the EUs with good channel status to maximize the EE,

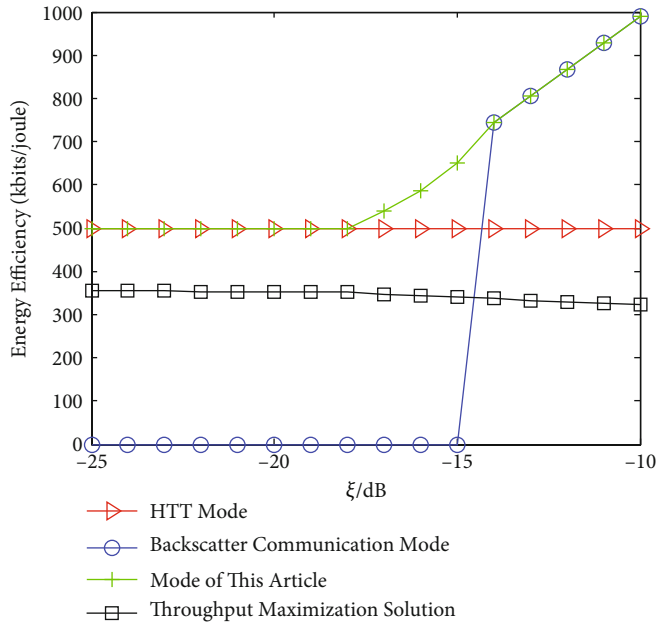

Figure 4: Performance comparison of the four resource allocation schemes.

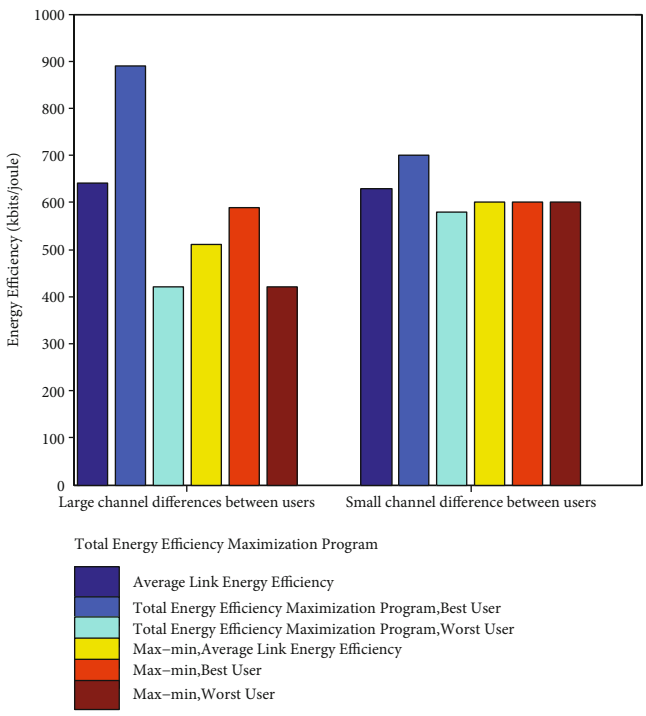

Figure 5: Comparison of the fairness of the two resource allocation options.

while the max–min scheme maximizes the EE of EUs with the worst link status to ensure fairness. As a result, the max–min scheme achieves much fairness at the sacrifice of less total EE.

5. Conclusion

This paper introduces a BAWPCN to address the energy shortage of sensor nodes due to frequent data interactions in digital twin workshops and proposes a resource allocation scheme to guarantee fairness in link EE. Considering the EUs' minimum rate requirement and energy causality constraints, the max–min system link EE optimization problem was formulated as a mixed-integer nonconvex fractional programming problem with time-power two-dimension resource joint optimization. By introducing generalized fractional theory, relaxation variables, BCD, and auxiliary variables, an iterative algorithm is designed to solve the transformation problem to obtain the resource allocation scheme. Finally, the following three conclusions are verified by simulation: (1) the proposed iterative algorithm can quickly converge and (2) the proposed resource allocation scheme can effectively guarantee the fairness of link EE.

Appendix

In the optimization problem (14), the objective function, constraints C1-C4 and C7 are linear, so we only need to prove that constraints C5 and C8 are convex constraints. In C5 and C8, $B_0\tau_m \log_2(1+\xi P_{\tau_m}(P_0^{(l)})/\sigma^2)$ and $p_{m,c}^{\text{Back}}\tau_m + p_{m,c}^{\text{HTT}} t_m + x_m$ are linear, so that a sufficient condition for the optimization problem (14) to be convex is that the Hessian matrix is $t_m \log_2(1+x_m|h_m|^2/t_m\sigma^2)$ seminegative definite. Construct the function $f = t_m \log_2(1+x_m|h_m|^2/t_m\sigma^2)$, and its Hessian matrix can be expressed as follows:

$$\nabla f^2 = \begin{bmatrix} -\frac{t_m|h_m|^4}{\sigma^4 \ln 2}\left(t_m + \frac{x_m|h_m|^2}{\sigma^2}\right)^{-2} & \frac{x_m|h_m|^4}{\sigma^4 \ln 2}\left(t_m + \frac{|h_m|^2 x_m}{\sigma^2}\right)^{-2} \\ \frac{x_m|h_m|^4}{\sigma^4 \ln 2}\left(t_m + \frac{|h_m|^2 x_m}{\sigma^2}\right)^{-2} & -\frac{x_m|h_m|^4}{t_m\sigma^4 \ln 2}\left(t_m + \frac{x_m|h_m|^2}{\sigma^2}\right)^{-2} \end{bmatrix}. \tag{A.1}$$

The first-order determinant of the Hesse matrix shown in formula (A.1) is less than 0, and the second-order determinant is equal to 0, so the Hesse matrix is a seminegative definite matrix. Therefore, both constraints C5 and C8 are convex constraints. Based on the above analysis, Lemma 1 is proved to be right.

Data Availability

The simulation data used to support the findings of this study are included within the article. The code used to support the findings of this study are available from the corresponding author upon request.

Conflicts of Interest

The authors declare that they have no conflicts of interest.

References

[1] F. Tao, Q. Qi, L. Wang, and A. Y. C. Nee, "Digital twins and cyber–physical systems toward smart manufacturing and industry 4.0: correlation and comparison," *Engineering*, vol. 5, no. 4, pp. 653–661, 2019.

[2] L. Wright and S. Davidson, "How to tell the difference between a model and a digital twin," *Advanced Modeling and Simulation in Engineering Sciences*, vol. 7, no. 1, pp. 1–13, 2020.

[3] T. H. Q. Qi, F. Tao, T. Hu et al., "Enabling technologies and tools for digital twin," *Journal of Manufacturing Systems*, vol. 58, pp. 3–21, 2021.

[4] Y. Ye, L. Shi, X. Chu, and G. Lu, "On the outage performance of ambient backscatter communications," *IEEE Internet of Things Journal*, vol. 7, no. 8, pp. 7265–7278, 2020.

[5] H. Ju and R. Zhang, "Throughput maximization in wireless powered communication networks," *IEEE Transactions on Wireless Communications*, vol. 13, no. 1, pp. 418–428, 2014.

[6] X. Kang, C. K. Ho, and S. Sun, "Full-duplex wireless-powered communication network with energy causality," *IEEE Transactions on Wireless Communications*, vol. 14, no. 10, pp. 5539–5551, 2015.

[7] D. Kuester and Z. Popovic, "How good is your tag?: Rfid backscatter metrics and measurements," *IEEE Microwave Magazine*, vol. 14, no. 5, pp. 47–55, 2013.

[8] R. J. Vyas, B. B. Cook, Y. Kawahara, and M. M. Tentzeris, "E-WEHP: a batteryless embedded sensor-platform wirelessly powered from ambient digital-tv signals," *IEEE Transactions on Microwave Theory and Techniques*, vol. 61, no. 6, pp. 2491–2505, 2013.

[9] N. Van Huynh, D. T. Hoang, X. Lu, D. Niyato, P. Wang, and D. I. Kim, "Ambient backscatter communications: a contemporary survey," *IEEE Communication Surveys and Tutorials*, vol. 20, no. 4, pp. 2889–2922, 2018.

[10] D. T. Hoang, D. Niyato, P. Wang, D. I. Kim, and Z. Han, "Ambient backscatter: a new approach to improve network performance for rf-powered cognitive radio networks," *IEEE Transactions on Communications*, vol. 65, no. 9, pp. 3659–3674, 2017.

[11] B. Lyu, H. Guo, Z. Yang, and G. Gui, "Throughput maximization for hybrid backscatter assisted cognitive wireless powered radio networks," *IEEE Internet of Things Journal*, vol. 5, no. 3, pp. 2015–2024, 2018.

[12] P. Ramezani and A. Jamalipour, "Optimal resource allocation in backscatter assisted wpcn with practical energy harvesting model," *IEEE Transactions on Vehicular Technology*, vol. 68, no. 12, pp. 12406–12410, 2019.

[13] S. Xiao, H. Guo, and Y.-C. Liang, "Resource allocation for full-duplex-enabled cognitive backscatter networks," *IEEE Transactions on Wireless Communications*, vol. 18, no. 6, pp. 3222–3235, 2019.

[14] G. Yang, X. Xu, and Y.-C. Liang, "Resource allocation in noma-enhanced backscatter communication networks for wireless powered iot," *IEEE Wireless Communications Letters*, vol. 9, no. 1, pp. 117–120, 2020.

[15] L. Shi, R. Q. Hu, J. Gunther, Y. Ye, and H. Zhang, "Energy efficiency for rf-powered backscatter networks using htt protocol," *IEEE Transactions on Vehicular Technology*, vol. 69, no. 11, pp. 13932–13936, 2020.

[16] H. Yang, Y. Ye, X. Chu, and S. Sun, "Energy efficiency maximization for uav-enabled hybrid backscatter-harvest-then-transmit communications," *IEEE Transactions on Wireless Communications*, vol. 21, no. 5, pp. 2876–2891, 2022.

[17] E. Boshkovska, D. W. K. Ng, N. Zlatanov, and R. Schober, "Practical non-linear energy harvesting model and resource allocation for swipt systems," *IEEE Communications Letters*, vol. 19, no. 12, pp. 2082–2085, 2015.

[18] S. H. Kim and D. I. Kim, "Hybrid backscatter communication for wireless-powered heterogeneous networks," *IEEE Transactions on Wireless Communications*, vol. 16, no. 10, pp. 6557–6570, 2017.

[19] M. Ismail, W. Zhuang, E. Serpedin, and K. Qaraqe, "A survey on green mobile networking: from the perspectives of network operators and mobile users," *IEEE Communication Surveys and Tutorials*, vol. 17, no. 3, pp. 1535–1556, 2015.

[20] H. Yang, Y. Ye, and X. Chu, "Max-min energy-efficient resource allocation for wireless powered backscatter networks," *IEEE Wireless Communications Letters*, vol. 9, no. 5, pp. 688–692, 2020.

[21] M. Hong, M. Razaviyayn, Z.-Q. Luo, and J.-S. Pang, "A unified algorithmic framework for block-structured optimization involving big data: with applications in machine learning and signal processing," *IEEE Signal Processing Magazine*, vol. 33, no. 1, pp. 57–77, 2016.

[22] Y. Xu and W. Yin, "A block coordinate descent method for regularized multiconvex optimization with applications to nonnegative tensor factorization and completion," *SIAM Journal on Imaging Sciences*, vol. 6, no. 3, pp. 1758–1789, 2015.

[23] M. Razaviyayn, M. Hong, and Z. Q. Luo, "A unified convergence analysis of block successive minimization methods for nonsmooth optimization," *SIAM Journal on Optimization*, vol. 23, no. 2, pp. 1126–1153, 2012.